Chemistry–A European Journal
Research Article
doi.org/10.1002/chem.202301244
Chemistry Europe
European Chemical Societies Publishing
www.chemeurj.org

Substitution Effects on the Photophysical and Photoredox Properties of Tetraaza[7]helicenes

Johannes Rocker,[a] Johannes A. Dresel,[a] Leonie A. Krieger,[a] Paul Eckhardt,[a] Ana M. Ortuño,[b] Winald R. Kitzmann,[a] Guido H. Clever,[b] Katja Heinze,[a] and Till Opatz*[a]

Abstract: A series of substituted derivatives of tetraaza[7]helicenes were synthesized and the influence of the substitution on their photophysical and photoredox-catalytic properties was studied. The combination of their high fluorescence quantum yields of up to 0.65 and their circularly polarized luminescence (CPL) activity results in CPL brightness values (B_{CPL}) that are among the highest recorded for [7]helicenes so far. A sulfonylation/hetarylation reaction using cyanopyridines as substrates for photoinduced electron transfer (PET) from the excited helicenes was conducted to test for viability in photoredox catalysis. DFT calculations predict the introduction of electron withdrawing substituents to yield more oxidizing catalysts.

Introduction

The research interest in helicenes has grown in recent years, driven by the increasing number of synthetic approaches[1–8] and the desire to exploit the unique properties of this class of compounds, which originate from their helical structure in combination with the extended aromatic system. Helicenes find a wide variety of applications, such as synthetic use in the preparation of chiral catalysts, often in the form of ligands, or more exotic applications including the construction of molecular machines. In particular, their (chir)optical properties are increasingly being highlighted in the current literature and are used, for example, in molecular sensors and switches.[9–14] Enantiopure helicenes exhibit strong circular dichroism, absorbing circularly left- and right-polarized light to different extents and emitting light with a preferential circular polarization upon excitation (circularly polarized luminescence, CPL).[15–16] Since the emission is not linked to a specific functional group or moiety (ketone, BODIPY), but originates from the helically bent acene backbone, substitution in and decoration of the core structure allows for a variety of modifications to tune the electronic and optical properties.[17] In order to compare the CPL activity of different compounds, the dissymmetry factor of emission (g_{lum}), defined as $2(I_L-I_R)/(I_L+I_R)$, is commonly used, with I_L and I_R being the intensity of light with left-handed and right-handed circular polarization, respectively. However, currently available CPL dyes show low g_{lum} values, and efforts are being made to increase them to ranges that make the dyes suitable for applications such as CPL microscopy, 3D displays, and CP-OLEDs.[9,18] Strategies for CPL enhancement include the introduction of host-guest interactions,[19] additional annulations,[20] or self-assembly of helical structures,[21] but can also be achieved by substitution of CPL emitters.[22–23]

Another field of application of light-absorbing organic molecules utilizes the absorbed photon energy to enable chemical transformations via photocatalysis. While the renaissance of photoredox chemistry was initially based on precious metal-based catalysts (Ru, Ir),[24–25] organic photocatalysts were rapidly included,[26–27] and their importance and applications continue to grow.[28–30] However, helicenes have not been broadly considered as potential photoredox catalysts, with the only reports to the best of our knowledge being the use of a helical carbenium ion by Gianetti et al.[31] and later Cozzi et al.[32] We recently investigated the use of a polyaza[7]helicene as a reductive photocatalyst[33] and here report a chromatography-free gram-scale synthesis of the catalyst and provide further insight into its optical properties. In addition, five substituted azahelicenes were synthesized and characterized with respect to their (chir)optical properties, and the influence of the substitution pattern on the catalytic performance was tested. DFT calculations of three additional model compounds draw a path for further optimization by introducing electron-withdrawing substituents.

Synthesis

The azahelicenes **7a–f** (Scheme 2) can be prepared in two steps from 2-chloroquinolines **3a–f**, of which **3a** and **3b** are

[a] J. Rocker, J. A. Dresel, L. A. Krieger, P. Eckhardt, W. R. Kitzmann, Prof. Dr. K. Heinze, Prof. Dr. T. Opatz
Department of Chemistry
Johannes Gutenberg-University
Duesbergweg 10–14, 55128 Mainz (Germany)
E-mail: opatz@uni-mainz.de
[b] Dr. A. M. Ortuño, Prof. Dr. G. H. Clever
Department of Chemistry and Chemical Biology
TU Dortmund University
Otto-Hahn-Str. 6, 44227 Dortmund (Germany)

Supporting information for this article is available on the WWW under https://doi.org/10.1002/chem.202301244

commercially available.[33–34] The 2-chloroquinolines **3c–f** (Scheme 1) with substituents in 6- and 8-position can be prepared in three steps from cinnamoyl chloride and the corresponding anilines. Aminolysis of the acid chloride yields anilides which were cyclized to the quinoline-2(1*H*)-ones in a Friedel-Crafts reaction with an excess of aluminum chloride either in chlorobenzene[35–36] or solvent-free in a melt,[37] leading to the elimination of benzene. Deoxychlorination with phosphoryl chloride gives the 2-chloroquinolines **3**. 2-Chloro-4-phenylquinoline **3c** was prepared in three steps from ethyl benzoylacetate.

Aminolysis to the anilide **4**,[38] cyclization to the quinoline-2(1*H*)-one in polyphosphoric acid[39] and refluxing in phosphoryl chloride gave **3c**. 2-Chloro-4-methylquinoline **2b** can be prepared analogously using sulfuric acid.[40] Azahelicenes were prepared from the 2-chloroquinolines analogously to the unsubstituted parent compound **7a** (Scheme 2) in a double nucleophilic aromatic substitution followed by oxidation with phenyliodine bis(trifluoroacetate) (PIFA).[33–34] For **7a** and the methyl-substituted **7b**, an alternative purification protocol avoiding column chromatography was used for gram-scale preparations, slightly reducing the yields obtained (53% **7a**, 62% **7b**) but efficiently removing impurities and discoloration.

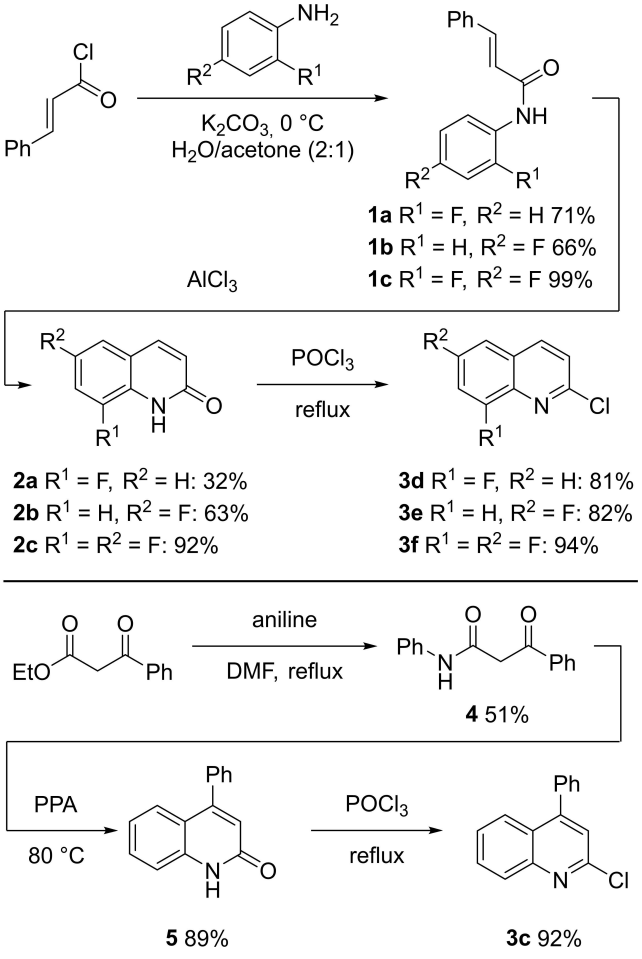

Scheme 1. Synthesis of the chloroquinolines **3c–f**.

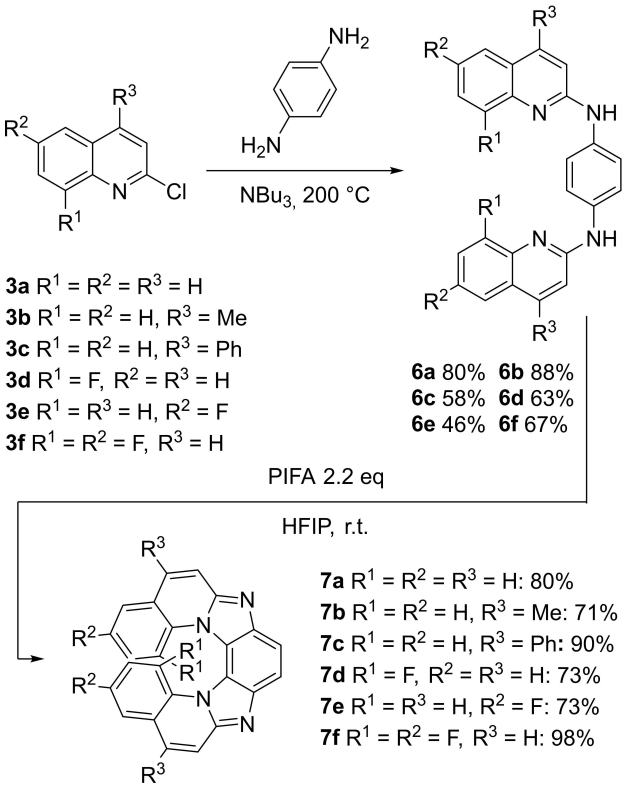

Scheme 2. Synthesis of the azahelicenes **7a–f** in two steps from chloroquinolines.

Single crystals suitable for X-ray diffractometry were grown by evaporation of solutions of **7c** in CH_2Cl_2/pentane. The structure (Figure 1) shows the helically bent shape of the molecule, in which the torsional angles of the inner atoms add up to 71.4° (9.6°, 26.9°, 4.2°, 24.4°, 6.3°), with most of the twisting on the two imidazole subunits.

Characterization of photophysical properties

Absorption and emission spectra were recorded in acetonitrile solution (Figure 2). The lowest energy absorption bands of **7a–f** tail into the blue spectral region and the broad fluorescence bands peak between 457 and 484 nm. Compared to the

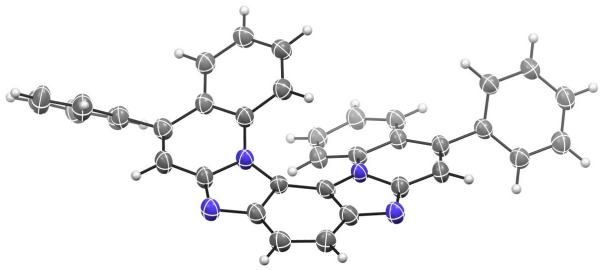

Figure 1. Molecular structure of **7c** determined by single crystal XRD on *rac*-**7c**, (*M*)-enantiomer shown. CCDC deposit number 2241858.

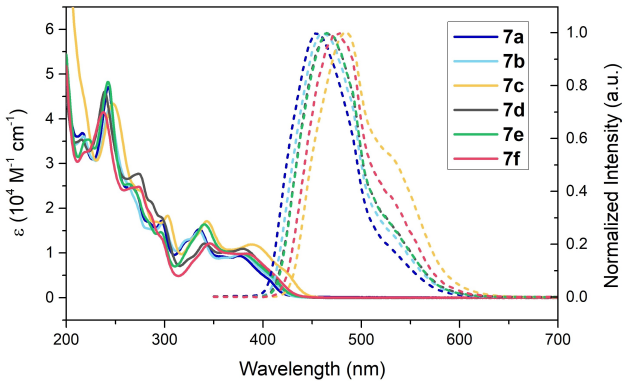

Figure 2. Absorption and emission spectra of **7a–f** in MeCN (20 μM) at room temperature.

unsubstituted helicene **7a**, the absorption and emission spectra of **7b–f** are red-shifted which is most pronounced for **7c**. This is due to their extended conjugated system (**7c**) and the fluorination (**7d–f**), respectively. The presence of excimers as a source of the shoulder at longer wavelengths was ruled out by measuring the fluorescence of **7c** at varying concentration, but no change in the spectrum was observed. Luminescence spectroscopy at 77 K reveals a fine structure of the fluorescence with three maxima in all cases (Table 1, Supporting Information Figure S7). Additionally, a weak, delayed emission between 525–650 nm was observed at low temperatures, which we assign to phosphorescence from excited triplet states. The corresponding triplet energies of 2.22–2.32 eV were determined from the lowest energy phosphorescence band maxima $\lambda_{max(ph)}$ (Table 3). The assignment as triplet states was confirmed by quenching experiments with O_2 forming $^1O_2$ (see below), which was detected via its emission signature at 1274 nm.[41] For **7b–d** and **7f** excitation spectra were recorded and closely follow the absorption spectra of the helicenes, confirming them as the source of the $^1O_2$ production (Figure S8).

High fluorescence quantum yields (Φ_{fl}) of 0.20-0.65 with nanosecond emission lifetimes τ were measured for **7a–f** in deaerated acetonitrile and dichloromethane (Table 1). Under deaerated conditions, fluorescence quantum yields for the fluorinated helicenes **7d** (29%) and **7f** (25%) are lower compared to the other azahelicenes including **7e**, whose Φ_{fl} remains above 40%. Halogenation often lowers the fluorescence quantum yield due to enhanced spin-orbit coupling, enabling higher intersystem crossing rates to the triplet state from which a non-radiative decay to the ground state occurs.[42–43] However, fluorine does not show this effect due to its low atomic number, and the effect of fluorination varies on a case-by-case basis for different fluorophores.[44–46] For the azahelicenes studied here, a fluorination in 1,16-position (**7d**) reduces Φ_{fl} to a greater extent than fluorination in 3,14-position (**7e** and **7f**). Φ_{fl} in dichloromethane are higher than in acetonitrile for **7a–d**, as is expected for a lower polarity solvent ($\varepsilon_{MeCN} = 36.64$ vs. $\varepsilon_{CH2Cl2} = 8.93$)[47] resulting in a decreased non-radiative decay rate.[48]

Under air, quenching by oxygen lowered Φ_{fl}, with quenching efficiencies in MeCN ranging from 20% for the tetrafluorinated **7f** to 35% for less-substituted **7a** and **7b** (SI, Table S1). The fluorescence lifetimes of **7a–f** also shorten in the presence of oxygen (Table S1) with quenching efficiencies matching those obtained from fluorescence quantum yields.

The (*P*)- and (*M*)-enantiomers of **7a–f** were resolved using semi-preparative HPLC with chiral stationary phases. Depending on the retention time differences and the solubility of the compounds, 3–10 mg could be purified in a single injection with stacked injections speeding up the separation of larger quantities. The purity of the separated enantiomers was assessed via analytical HPLC (SI, Figures S12–17). Optical rotations of the enantiomers were measured in chloroform and corrected for the determined enantiomeric excess (Table 2). The configurational stability and the activation parameters of enantiomerization of **7a–f** were determined by examining the

Table 1. Absorption maxima $\lambda_{max(abs)}$ and the corresponding molar extinction coefficients ε, fluorescence maxima $\lambda_{max(fl)}$, fluorescence quantum yields Φ_{fl}, fluorescence lifetimes τ_{fl} and phosphorescence maxima $\lambda_{max(ph)}$ for azahelicenes **7a–f**. Absorption (20 μM), fluorescence (20 μM) at room temperature and fluorescence lifetimes (100 μM) were measured in MeCN. Low temperature measurements were performed in EtOH/MeOH (4:1) glass at 100 μM concentration.

Compound	$\lambda_{max(abs)}$ [nm] (ε [10^3 $M^{-1}\cdot cm^{-1}$])		$\lambda_{max(fl)}$ [nm]		Φ_{fl} (degassed)[g]		τ_{fl} (ns) (degassed)[f,g]	$\lambda_{max(ph)}$ [nm][c]
	MeCN	CH_2Cl_2[a]	(r.t.)[b]	(77 K)[c]	MeCN[d]	CH_2Cl_2[e]	(r.t.)	(77 K)
7a	376 (9.4), 335 (15.3), 297 (17.2)	380 (10.2), 337 (16.8), 299 (17.6)	457	413, 436, 464	0.48	0.65	9.6	535, 577
7b	378 (9.8), 335 (14.8), 299 (16.9)	380 (16.8), 335 (24.6), 301 (28.0)	461	413, 437, 464	0.41	0.54	8.9	539
7c	389 (11.9), 343 (17.1), 303 (18.3)[a]	391 (19.9), 345 (27.9), 305 (29.1)	484[a]	436, 462, 488	0.53	0.64	6.9	558
7d	379 (10.9), 340 (12.1), 298 (17.7 sh)	383 (10.9), 345 (12.1), 299 (17.4 sh)	464	416, 441, 467	0.29	0.41	6.3	543, 588
7e	379 (9.8), 340 (16.4), 296 (14.7)	382 (13.9), 342 (23.5), 298 (19.6)	464	418, 442, 469	0.42	0.33	9.3	540, 581
7f	383 (9.9), 345 (12.1), 296 (13.6 sh)	388 (14.7), 350 (17.7), 298 (17.9 sh)	477	424, 448, 473	0.24	0.20	6.1	549, 593

[a] 10 μM. [b] $\lambda_{ex} = 250$ nm. [c] λ_{ex}: **7a** 340 nm; **7b** 333 nm; **7c** 345 nm; **7d** 340 nm; **7e** 336 nm; **7f** 333 nm. [d] 100 μM, λ_{ex}: 320 nm. [e] 10 μM, **7a** 337 nm; **7b** 335 nm; **7c** 345 nm; **7d** 345 nm; **7e** 342 nm; **7f** 350 nm. [f] λ_{ex}: 395 nm. [g] estimated relative error: 5%.

Table 2. Optical rotations [α], emission dissymmetry factors g_{lum}, CPL brightness B_{CPL}, enthalpy $\Delta H^{\ddagger}$, entropy $\Delta S^{\ddagger}$, and free enthalpy $\Delta G^{\ddagger}$ of enantiomerization and enantiomer lifetimes τ_e of azahelicenes **7a–f**.

Compound		$[\alpha]_D^{23}$ [10^3° cm^3 g^{-1} dm^{-1}][a] (enantiomeric excess)	g_{lum} (10^{-3})[b]	B_{CPL} [M^{-1} cm^{-1}][e]	Enantiomerization barrier[c] ΔH [kcal/mol]	$\Delta S^{\ddagger}$ [cal/mol]	$G^{\ddagger}_{348\,K}$ [kcal/mol][d]	$\tau_{e,348\,K}$ [h]
7a	(*P*)	+3000 ± 200 (0.998)	8.1	44 ± 2	22.6 ± 1.8	−16.6 ± 5.4	28.2 ± 0.0	37.8 ± 0.6
	(*M*)	−3300 ± 200 (0.994)	−8.1	(Lit.: 37.6)[34,52]				
7b	(*P*)	+3300 ± 200 (0.979)	6.7	45 ± 2	29.0 ± 3.5	3 ± 11	27.9 ± 0.0	25.5 ± 0.2
	(*M*)	−3400 ± 200 (0.993)	−6.9					
7c	(*P*)	+2300 ± 100 (0.985)	3.1	27 ± 2	23.6 ± 1.3	−11.1 ± 3.9	27.4 ± 0.0	12.7 ± 0.6
	(*M*)	−1800 ± 100 (0.959)	−2.9					
7d	(*P*)	+2900 ± 100 (0.991)	6.6	14 ± 2	31.3 ± 0.5	−3.3 ± 1.4	32.5 ± 0.0	18000 ± 200
	(*M*)	−2400 ± 100 (0.999)	−5.1					
7e	(*P*)	+3200 ± 200 (0.998)	7.3	29 ± 1	23.7 ± 1.2	−12.6 ± 3.6	28.0 ± 0.0	29.7 ± 0.1
	(*M*)	−2800 ± 100 (0.987)	−7.4					
7f	(*P*)	+3500 ± 200 (> 0.999)	6.5	11 ± 1	33.4 ± 2.1	3.3 ± 5.9	32.3 ± 0.0	14400 ± 70
	(*M*)	−3400 ± 200 (> 0.999)	−6.4					

[a] $c = 0.05$ in $CHCl_3$, a relative error of 5% is assumed. [b] in CH_2Cl_2 at $\lambda_{max(fl)}$, λ_{exc} **7a** 337 nm; **7b** 335 nm; **7c** 345 nm; **7d** 345 nm; **7e** 343 nm; **7f** 350 nm. [c] in ^{n}AmylOH [d] errors were in the range of 9–13 cal/mol. [e] ε at the excitation wavelength of the CPL measurement and Φ_{fl} in CH_2Cl_2 are used for calculation. The mean value of g_{lum} was used to calculated the CPL brightness; error is calculated by propagation of error assuming $^1/_2\Delta g_{lum}$ as the error of g_{lum} and a relative error of 5% for Φ_{fl}.

racemization ($k_{rac} = 2k_e$) via HPLC at constant temperatures over time (see Supporting Information for further information).

Specific optical rotatory powers of the helicenes range from +2300° cm^3 g^{-1} dm^{-1} ((*P*)-**7c**) to +3555° cm^3 g^{-1} dm^{-1} ((*P*)-**7f**). The assignment of absolute configuration is based on the general relationship that (*P*)-helicenes are dextrorotatory and (*M*)-helicenes are levorotatory,[9–10] and was confirmed exemplarily by DFT calculation of the ECD spectrum of **7a** (Figure S18). The activation parameters of enantiomerization of the aza[7]helicenes (Table 2) show the expected effect of increased conformational stability for C-1 substituted derivatives (**7c**, **7f**). The influence of temperature on $\Delta G^{\ddagger}$ is small as was reported for carbon[*n*]helicenes.[49] The values of $\Delta G^{\ddagger}$ calculated for **7a–f** lie between those of carbo[5]helicene (24.1 kcal/mol (298 K))[49] and carbo[6]helicene (35.4 kcal/mol (298 K))[49] and are lower than for [7]helicenes consisting only of six-membered rings, since the presence of the two five-membered rings drastically lowers the enantiomerization barrier.[9,49] The influence of the substituents in 3,14- and 5,12-position is much smaller, but the phenyl substituents in **7c** slightly lower the barrier of enantiomerization compared to the unsubstituted structure. It should be noted that the phenyl rings in **7c** are not fully conjugated to the π-system of the helix, as the planar configuration of the phenyl substituents is expected to be hindered to a similar extent as in 1-phenylnaphthalene.[50–51] An equilibrium torsion angle of 50–70°, depending on the solvent, has been reported for 1-phenylnaphthalene,[51] and an appropriate angle is observed in the crystal structure of *rac*-**7c** (Figure 1, additionally see Supporting Information, CCDC deposit number 2241858).

ECD-spectra of compounds **7a–f** were recorded in dichloromethane solution and are shown in Figure 3. The (*P*)-enantiomers of the azahelicenes show positive Cotton bands at longer wavelengths. The 1,16-substituted **7d** and **7f** have less structured spectra compared to the compounds without substituents at this position, resulting in differences in the region around 330 nm. The spectra of the (*M*)-enantiomers appear as mirror images. A plot of the dissymmetry factor of absorption (g_{abs}) is given in the Supporting Information (Figure S19).

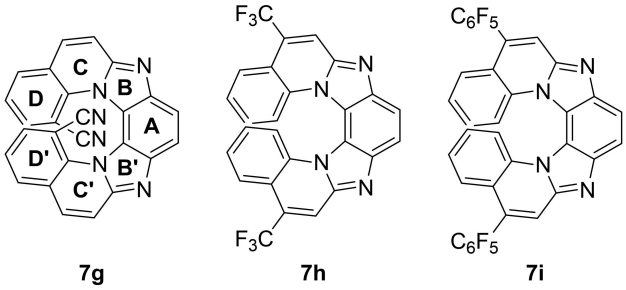

Figure 3. ECD-spectra (top, 100 μM, d = 1 mm) and 2Δ*I*-spectra of emission (bottom, 25 μM) of **7a–f** in CH_2Cl_2. Solid lines: (*P*)-(+)-Enantiomers, dashed lines: (*M*)-(−)-Enantiomers.

Circulary polarized luminescence (CPL) spectra were recorded (Figure 3) and the dissymmetry values g_{lum} at $\lambda_{max,em}$ are given in Table 2. The absolute g_{lum} values for the (*P*)- and (*M*)-enantiomers match for each compound, except for **7d**, showing a lower value for the (*M*)-enantiomer. A difference was also observed in the optical rotation in this case. The differences for the enantiomers of **7d** may result from a luminescent impurity which cannot be removed in this particular case via the chromatography methods applied, which can be detected in the absorption and emission spectra of the two enantiomers (see Supporting Information, Figures S20, S21). Substitution lowers the CPL intensity and the unsubstituted **7a** remains the strongest CPL emitter in this series of helicenes with $|g_{lum}| = -8.1 \cdot 10^{-3}$, which is consistent with the value determined by Otani et al.[34] To allow for a direct comparison to other CPL-emitters, the CPL brightness (B_{CPL}), which was introduced by Arrico et al., was calculated using the molar extinction coefficient at excitation wavelength and the fluorescence quantum

yield of each helicene using Equation (1).[52] For the calculation, $|g_{lum}|$ was defined as the mean of the g_{lum} absolute values for the (*P*)- and (*M*)-enantiomers.

$$B_{CPL} = {}^{1}/_{2}\ \varepsilon_{\lambda} \cdot \Phi_{fl} \cdot |g_{lum}| \quad (1)$$

The azahelicenes **7a–f** show exceptionally high B_{CPL} values of 11.4–45.0 $M^{-1}cm^{-1}$ at the excitation wavelength used for CPL measurements (see Table 2, Footnote [b]). For **7a** the value we obtained is higher than in earlier reports (B_{CPL} = 37.6)[52] due to the higher fluorescence quantum yield determined in our measurement. The increased extinction coefficient of **7b** yields a higher CPL brightness compared to **7a**, despite its lower fluorescence quantum yield and dissymmetry factor g_{lum}. The CPL brightness of B_{CPL} = 45 $M^{-1}cm^{-1}$ for **7b** is among the highest of [7]helicenes compiled by Arrico et al., with only few, mostly dimeric, helicenes showing higher values.[52]

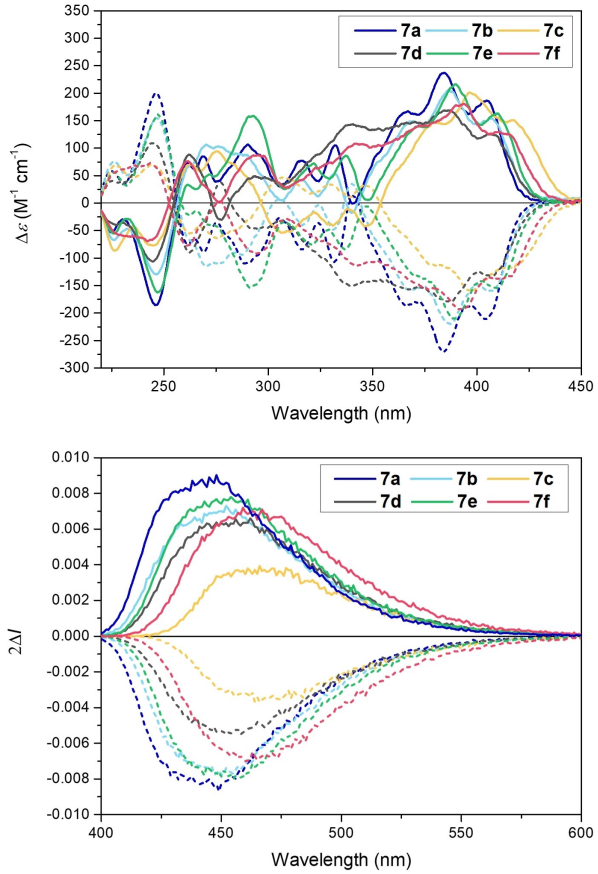

Figure 4. Structures of model compounds **7g–7i** and exemplary annotation of the ring system.

Photocatalytic properties

To explore the electronic structure of the azahelicenes and the effect of substitution DFT calculations were performed on the structures **7a–f** and additionally on model compounds **7g–i** (Figure 4) to investigate the influence of stronger acceptor substituents.

Calculated HOMO- and LUMO energies are included in Table 3 and the frontier orbitals are shown in the Supporting Information. Attachment of a methyl or phenyl group in 5,12-position destabilizes the HOMO by +0.14 eV and +0.12 eV, respectively. Placing a CF_3-group or a C_6F_5-group in the same position (model substrates **7h**, **7i**) results in a strong stabilization compared to the non-fluorinated substituents (−0.71 eV $CH_3 \rightarrow CF_3$, −0.47 eV $Ph \rightarrow C_6F_5$). The LUMO energy of the methylated **7b** is raised to a similar extent (+0.11 eV) as the HOMO, resulting in comparable absorption and emission bands of **7a** and **7b** but an easier oxidation of **7b**. Fluorination on the inner ring positions (1,16) does not influence the HOMO level but fluorination in the 3,14-position stabilizes it by −0.23 eV. LUMOs of the fluorinated derivatives **7d** and **7e** are shifted similarly to the HOMOs, with the 1,16-F-substitution having a lesser stabilizing effect compared to the 3,14-substitution (−0.06 eV and −0.27 eV). Orbitals of the tetrafluorinated helicene **7f** show the combined effect of both substitutions. In model substrate **7g** the cyano group in 1,16-position, unlike a fluoro-substitution, does stabilize (−0.17 eV) the HOMO but is also predicted to stabilize the LUMO to an even larger extent (−0.51 eV) leading to a reduced energy gap of 3.23 eV.

The HOMO is predominantly localized on the central A-, B- and C-rings, while the LUMO mainly extends to the outer (C- and D-) rings. The substituents only have minor effects on the orbital coefficients of the HOMOs. The LUMO of **7c** and **7i** is extended to the phenyl rings to a small extent while the orbital coefficients in the D-rings are smaller, in contrast to the LUMO

Table 3. Excited state energies, redox potentials and HOMO–LUMO energies of azahelicenes **7a–f**. Estimated values from HOMO–LUMO energies for **7g–i** are given in italics.

Helicene	**7a**	**7b**	**7c**	**7d**	**7e**	**7f**	**7g** (oCN)	**7h** (CF_3)	**7i** (PFP)
$E_{0,0}$ (eV)	2.98	2.95	2.84	2.92	2.94	2.88	*2.64*	*2.87*	*2.77*
E_T (eV)[b]	2.32	2.30	2.22	2.28	2.30	2.26	–	–	–
$E_{1/2,ox}$ (V)	1.15	1.08	1.10	1.21	1.28[a]	1.33	*1.32*	*1.72*	*1.50*
E^{*}_{Ox} (V)	−1.83	−1.87	−1.74	−1.71	−1.66	−1.55	*−1.32*	*−1.15*	*−1.26*
HOMO (eV)	−5.53	−5.39	−5.41	−5.52	−5.76	−5.74	−5.70	−6.10	−5.88
LUMO (eV)	−1.96	−1.85	−2.01	−2.02	−2.24	−2.30	−2.47	−2.64	−2.53
calc. HOMO-LUMO gap (eV)	3.57	3.54	3.40	3.50	3.52	3.44	3.23	3.46	3.35

All potentials are given vs. SCE. Cyclic voltammetry, as well as absorption and emission spectra were recorded in CH_2Cl_2. [a] No reversible reduction was observed, the peak potential is used. [b] From lowest $\lambda_{max(ph)}$.

coefficients of the cyano-substituted **7g**, which are larger on the outer D-rings compared to any other derivative studied here. The calculations allow prediction of the (photo)redox and optical properties of the model substrates, and the estimated values are given in Table 3. Further information on the calculations of the excited state energies and redox potentials is given in the Supporting Information.

To estimate the photoredox potentials of the catalysts **7a–f** cyclic voltammograms were recorded (SI, Figure S9). Using the equation for the Gibbs energy of photoinduced electron transfer (Eq. (2)), omitting the electrostatic work term, the excited state potentials of the helicenes were calculated. The excited state energy $E_{0,0}$ is approximated from the absorption and fluorescence spectra using the midpoint between the lowest energy absorption maximum and the fluorescence maximum.[26] The potentials are compiled in Table 3.

$$E^{*}_{Ox}(PC^{\bullet+}/PC^{*}) = E_{Ox}(PC^{\bullet+}/PC) - E_{0,0} \quad (2)$$

The oxidation potentials of the fluorinated helicenes **7d–f** are increased compared to the donor-substituted or unsubstituted helicenes **7a–c**, as expected for electronegative substituents. The effect is not very pronounced due to the strong mesomeric properties of the fluorine substituents which attenuate the inductive effect (resonance parameter $R = -0.39$, field effect parameter $F = 0.45$).[53] The methyl- (**7b**, $R = -0.18$, $F = 0.01$)[53] and phenyl-substituted (**7c**, $R = -0.13$, $F = 0.12$)[53] derivatives show a comparable oxidation potential, while the excited state energy of **7c** is decreased as the extended π-system reduces the HOMO–LUMO gap. **7c** shows a second oxidation wave ($E_{1/2,ox,2} = +1.37$ V) with both oxidations being reversible. Apart from this, reversibility of the first oxidation on the CV time scale was observed only for **7a** and **7f**. No peaks in the reductive region were observed except for **7f** (−1.58 V), which corresponds to an electrochemical gap of 2.91 eV that compares well to the estimated optical gap $E_{0,0} = 2.88$ eV. The expected position of the reductive peaks for **7a–e** is beyond the potential window of dichloromethane and sweeps to −2 V failed to give peaks in these cases. **7h** and **7i** are expected to show increased oxidation potentials compared to their non-fluorinated counterparts **7b** and **7i**. This effect is especially pronounced for **7h**, which should be a photoredox catalyst with a much lower reductive power in the excited state.

The photoredox-catalytic properties of **7a–f** were compared in a sulfonylation/hetarylation of styrenes earlier developed in our lab[54] using four different cyanopyridine substrates **8a–d** with varying reduction potentials. The results are compiled in Scheme 3. The stronger reducing derivatives **7a–c** give higher yields in this reaction compared to the fluorinated compounds **7d–f**, even if the catalyst's reduction potential matches or surpasses the substrates electron affinity by calculation as is the case for the combinations **7d–f** and **8a**. Another factor coming into play might be the singlet lifetime (Table 1) which is decreased for **7d** and **7f**. Certain combinations (**7d** and **8b**, **7e** and **8a**) give high yields of the product even if the catalyst's reduction potential should not allow for efficient electron transfer to the substrate.

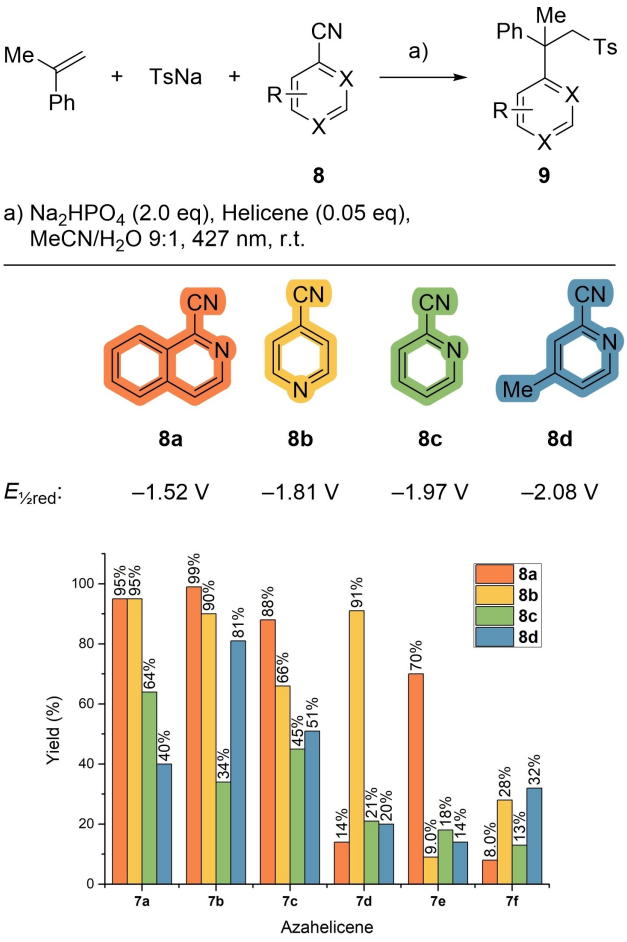

Scheme 3. Reaction conditions of the sulfonylation/arylation and the used cyanopyridines with their reduction potentials (in MeCN, vs SCE). The yields achieved with the helicenes **7a–7f** are given in the bar diagram.

It was anticipated that the improved performance in the reaction with **8d** of **7b** compared to **7a** may also stem from a decreased decomposition rate trough styrene addition due blocking of the 6,11-positions by methyl groups. A comparison of the decay in acetonitrile solution containing 40 equiv. α-methylstyrene reveals the opposite to be true as the decomposition rate constant, assuming first order kinetics, for **7b** ($k_{decomp} = 6.1 \pm 0.3 \cdot 10^{-4}\ s^{-1}$) is twice the rate constant of **7a** ($k_{decomp} = 2.7 \pm 0.1 \cdot 10^{-4}\ s^{-1}$). While the spectral shift of 2 nm (Table 1) between **7a** und **7b** does increase the spectral overlap with the used lamp for **7b** (Supporting Information, Figure S23) it does so only to a small extent and cannot be the sole cause of the accelerated decomposition observed. The lower fluorescence quantum yield of **7b** (41 % vs. 48 % for **7a**) may be an indication of a higher intersystem crossing rate to the triplet state, from which the reaction of the catalyst with the styrene probably proceeds to decomposition.

Conclusions

The synthesis of substituted aza[7]helicenes from 2-chloroquinolines in a two-step sequence was demonstrated for six derivatives and the oxidative cyclization with PIFA proved a reliable method for each of the substrates used. The photophysical properties of the azahelicenes were extensively studied, a weak phosphorescence and the sensitization of $^1O_2$ show the formation of a triplet state. The chiroptical properties of the helicenes were studied after chromatographic separation of the enantiomers. Electronic circular dichroism and circularly polarized luminescence spectra were recorded, giving g_{lum} values in the 10^{-3} range for each of the derivatives.

The suitability of the helicenes as photoredox catalysts was evaluated in view of their reductive power in a sulfonylation/hetarylation reaction with four benchmark cyanopyridine substrates. The strongly reductive variants **7a** and **7b** performed best in this reaction. Subtle differences in the catalyst structure result in significant effects on substrate preference. While the use of chiral catalysts of this type in enantioselective photocatalysis will be investigated, structural modifications may be required to ensure a sufficient enantiodiscrimination. The redox potentials of the helicenes were determined by cyclic voltammetry and the excited state potentials estimated. DFT calculations were performed to visualize the frontier orbitals and to evaluate three additional model compounds and calculate their expected redox potentials. The influence of the substitution on the localization of the HOMO and LUMO was small in the synthesized cases.

Experimental Section

Deposition Number 2241858 (for **7c**) contains the supplementary crystallographic data for this paper. These data are provided free of charge by the joint Cambridge Crystallographic Data Centre and Fachinformationszentrum Karlsruhe Access Structures service.

General procedure for the coupling of 2-chloroquinolines with *p*-phenylenediamine: p-Phenylenediamine (1.0 eq), the corresponding 2-chloroquinoline (2.0 eq) and tributylamine (4.0 eq) were placed in round bottom reaction tube with a magnetic stir bar and sealed with a septum. After exchanging the atmosphere with N_2 the tube was closed with a screw cap and heated to 200 °C over night. The mixture was diluted with EtOAc and washed with $NaCO_3$ soln. (1 M) and brine. After drying with Na_2SO_4 and evaporation the residue was recrystallized from toluene.

General procedure for the oxidation to azahelicenes: The helicene precursor was dissolved in HFIP and PIFA was added in portions (0.4 eq) every 30 min. After the last addition (2.0–2.4 equiv. are required) the mixture is stirred over night and diluted with CH_2Cl_2, then washed with $NaHCO_3$ soln. and $Na_2S_2O_3$ soln. and dried with Na_2SO_4. The crude product is evaporated onto silica and purified via flash chromatography (gradient CH_2Cl_2 to CH_2Cl_2/MeOH = 97.5 : 2.5, Isolera system).

Supporting Information

General information on the materials and methods used, characterization data, additional spectra and chromatograms are included in the Supporting Information.

Additional references cited within the Supporting Information.[55–94]

Acknowledgements

We thank Dr. Dieter Schollmeyer for X-ray crystal structure analysis and Dr. Robert Naumann for quantum yield measurements. We thank Elie Benchimol and Dr. Jacopo Tessarolo (both Dortmund) for help with the CPL measurements. W.R.K. is thankful for support from the German Academic Scholarship Foundation and for financial support by the Max Planck Graduate Center with the Johannes Gutenberg University (MPGC) and the Fonds der Chemischen Industrie (FCI) . This work was supported by the Deutsche Forschungsgemeinschaft (RE 1203/23-1 and RE 1203/23-2, HE 2778/10-2), through Germany's Excellence Strategy – EXC2033 – project number 390677874 – RESOLV and through grant INST 247/1018-1 FUGG to K.H. and T.O. Open Access funding enabled and organized by Projekt DEAL.

Conflict of Interests

The authors declare no conflict of interest.

Data Availability Statement

The data that support the findings of this study are available in the supplementary material of this article.

Keywords: circulary polarized luminescence · density functional calculations · fluorescence · helicenes · photoredox catalysis

[1] M. S. H. Salem, M. I. Khalid, M. Sako, K. Higashida, C. Lacroix, M. Kondo, R. Takishima, T. Taniguchi, M. Miura, G. Vo-Thanh, H. Sasai, S. Takizawa, *Adv. Synth. Catal.* **2023**, *365*, 373–380.
[2] L. Menduti, C. Baldoli, S. Manetto, M. Bolte, H.-W. Lerner, G. Longhi, C. Villani, E. Licandro, M. Wagner, *Angew. Chem. Int. Ed.* **2023**, *62*, e202215468.
[3] W. Fu, V. Pelliccioli, M. von Geyso, P. Redero, C. Böhmer, M. Simon, C. Golz, M. Alcarazo, *Adv. Mater.* **2023**, *35*, 2211279.
[4] J. Zhang, M. Simon, C. Golz, M. Alcarazo, *Isr. J. Chem.* **2022**, e202200043.
[5] N. Terada, K. Uematsu, R. Higuchi, Y. Tokimaru, Y. Sato, K. Nakano, K. Nozaki, *Chem. Eur. J.* **2021**, *27*, 9342–9349.
[6] H. Oyama, M. Akiyama, K. Nakano, M. Naito, K. Nobusawa, K. Nozaki, *Org. Lett.* **2016**, *18*, 3654–3657.
[7] M. Gingras, G. Félix, R. Peresutti, *Chem. Soc. Rev.* **2013**, *42*, 1007–1050.
[8] M. Gingras, *Chem. Soc. Rev.* **2013**, *42*, 968–1006.
[9] C.-F. Chen, Y. Shen, *Helicene Chemistry*, Springer Berlin, Heidelberg **2017**.
[10] Y. Shen, C.-F. Chen, *Chem. Rev.* **2012**, *112*, 1463–1535.
[11] M. Gingras, *Chem. Soc. Rev.* **2013**, *42*, 1051–1095.
[12] F. Fontana, B. Bertolotti, *Molecules* **2022**, *27*, 2522.

[13] J. R. Brandt, L. Pospíšil, L. Bednárová, R. C. da Costa, A. J. P. White, T. Mori, F. Teplý, M. J. Fuchter, *Chem. Commun.* **2017**, *53*, 9059–9062.
[14] J. R. Brandt, X. Wang, Y. Yang, A. J. Campbell, M. J. Fuchter, *J. Am. Chem. Soc.* **2016**, *138*, 9743–9746.
[15] M. Cei, L. Di Bari, F. Zinna, *Chirality* **2023**, *35*, 192–210.
[16] J. M. dos Santos, D. Sun, J. M. Moreno-Naranjo, D. Hall, F. Zinna, S. T. J. Ryan, W. Shi, T. Matulaitis, D. B. Cordes, A. M. Z. Slawin, D. Beljonne, S. L. Warriner, Y. Olivier, M. J. Fuchter, E. Zysman-Colman, *J. Mater. Chem. C* **2022**, *10*, 4861–4870.
[17] H. Kubo, T. Hirose, T. Nakashima, T. Kawai, J.-y. Hasegawa, K. Matsuda, *J. Phys. Chem. Lett.* **2021**, *12*, 686–695.
[18] E. M. Sánchez-Carnerero, A. R. Agarrabeitia, F. Moreno, B. L. Maroto, G. Muller, M. J. Ortiz, S. de la Moya, *Chem. Eur. J.* **2015**, *21*, 13488–13500.
[19] K. Wu, J. Tessarolo, A. Baksi, G. H. Clever, *Angew. Chem. Int. Ed.* **2022**, *61*, e202205725.
[20] Y. Liu, Z. Ma, Z. Wang, W. Jiang, *J. Am. Chem. Soc.* **2022**, *144*, 11397–11404.
[21] Y.-X. Yuan, M. Hu, K.-R. Zhang, T.-T. Zhou, S. Wang, M. Liu, Y.-S. Zheng, *Mater. Horiz.* **2020**, *7*, 3209–3216.
[22] J.-T. Lin, D.-G. Chen, L.-S. Yang, T.-C. Lin, Y.-H. Liu, Y.-C. Chao, P.-T. Chou, C.-W. Chiu, *Angew. Chem. Int. Ed.* **2021**, *60*, 21434–21440.
[23] J. Gong, R. Huang, C. Wang, Z. Zhao, B. Z. Tang, X. Zhang, *Sens. Actuators B* **2021**, *347*, 130610.
[24] C. K. Prier, D. A. Rankic, D. W. C. MacMillan, *Chem. Rev.* **2013**, *113*, 5322–5363.
[25] D. Staveness, I. Bosque, C. R. J. Stephenson, *Acc. Chem. Res.* **2016**, *49*, 2295–2306.
[26] N. A. Romero, D. A. Nicewicz, *Chem. Rev.* **2016**, *116*, 10075–10166.
[27] Y. Du, R. M. Pearson, C.-H. Lim, S. M. Sartor, M. D. Ryan, H. Yang, N. H. Damrauer, G. M. Miyake, *Chem. Eur. J.* **2017**, *23*, 10962–10968.
[28] J. Lyu, M. Leone, A. Claraz, C. Allain, L. Neuville, G. Masson, *RSC Adv.* **2021**, *11*, 36663–36669.
[29] C. Prentice, J. Morrison, A. D. Smith, E. Zysman-Colman, *Chem. Eur. J.* **2023**, *29*, e202202998.
[30] H. Yue, C. Zhu, M. Rueping, *Sci. Bull.* **2023**, *68*, 367–369.
[31] L. Mei, J. M. Veleta, T. L. Gianetti, *J. Am. Chem. Soc.* **2020**, *142*, 12056–12061.
[32] F. Calogero, G. Magagnano, S. Potenti, F. Pasca, A. Fermi, A. Gualandi, P. Ceroni, G. Bergamini, P. G. Cozzi, *Chem. Sci.* **2022**, *13*, 5973–5981.
[33] J. Rocker, T. Opatz, *ACS Org. Inorg. Au* **2022**, *2*, 415–421.
[34] T. Otani, T. Sasayama, C. Iwashimizu, K. S. Kanyiva, H. Kawai, T. Shibata, *Chem. Commun.* **2020**, *56*, 4484–4487.
[35] M. C. Elliott, S. V. Wordingham, *Synlett* **2004**, *05*, 0898–0900.
[36] T.-C. Wang, Y.-L. Chen, K.-H. Lee, C.-C. Tzeng, *Synthesis* **1997**, *01*, 87–90.
[37] S. R. Inglis, C. Stojkoski, K. M. Branson, J. F. Cawthray, D. Fritz, E. Wiadrowski, S. M. Pyke, G. W. Booker, *J. Med. Chem.* **2004**, *47*, 5405–5417.
[38] F. M. Abdelrazek, Y. M. Elkholy, A. M. Salah, N. M. Abdelazeem, P. Metz, *J. Heterocycl. Chem.* **2014**, *51*, 824–829.
[39] L.-J. Huang, M.-C. Hsieh, C.-M. Teng, K.-H. Lee, S.-C. Kuo, *Bioorg. Med. Chem.* **1998**, *6*, 1657–1662.
[40] W. M. Lauer, C. E. Kaslow, *Org. Synth.* **1944**, *24*, 68–69.
[41] M. C. DeRosa, R. J. Crutchley, *Coord. Chem. Rev.* **2002**, *233–234*, 351–371.
[42] J. W. Verhoeven, *Pure Appl. Chem.* **1996**, *68*, 2223–2286.
[43] E. A. Slyusareva, F. N. Tomilin, A. G. Sizykh, E. Y. Tankevich, A. A. Kuzubov, S. G. Ovchinnikov, *Opt. Spectrosc.* **2012**, *112*, 671–678.
[44] M. A. H. Alamiry, A. C. Benniston, J. Hagon, T. P. L. Winstanley, H. Lemmetyinen, N. V. Tkachenko, *RSC Adv.* **2012**, *2*, 4944–4950.
[45] M. Bracker, M. K. Kubitz, C. Czekelius, C. M. Marian, M. Kleinschmidt, *ChemPhotoChem* **2022**, *6*, e202200040.
[46] A. Reiffers, C. Torres Ziegenbein, A. Engelhardt, R. Kühnemuth, P. Gilch, C. Czekelius, *Photochem. Photobiol.* **2018**, *94*, 667–676.
[47] W. M. Haynes, *CRC Handbook of Chemistry and Physics*, CRC Press **2016**.
[48] J. R. Lakowicz, *Principles of Fluorescence Spectroscopy* (Ed.: J. R. Lakowicz), Springer US, Boston, MA, **1983**, pp. 187–215.
[49] P. Ravat, *Chem. Eur. J.* **2021**, *27*, 3957–3967.
[50] R. D. Chirico, W. V. Steele, A. F. Kazakov, *J. Chem. Thermodyn.* **2014**, *73*, 241–254.
[51] D. Nori-shargh, S. Asadzadeh, F.-R. Ghanizadeh, F. Deyhimi, M. M. Amini, S. Jameh-Bozorghi, *J. Mol. Struct.* **2005**, *717*, 41–51.
[52] L. Arrico, L. Di Bari, F. Zinna, *Chem. Eur. J.* **2021**, *27*, 2920–2934.
[53] C. Hansch, A. Leo, R. W. Taft, *Chem. Rev.* **1991**, *91*, 165–195.
[54] B. Lipp, L. M. Kammer, M. Kücükdisli, A. Luque, J. Kühlborn, S. Pusch, G. Matulevičiūtė, D. Schollmeyer, A. Šačkus, T. Opatz, *Chem. Eur. J.* **2019**, *25*, 8965–8969.
[55] C. Ding, S. Li, K. Feng, C. Ma, *Green Chem.* **2021**, *23*, 5542–5548.
[56] J. Choi, H. Kim, *J. Chem. Theory Comput.* **2021**, *17*, 767–776.
[57] J. Corpas, P. Mauleón, R. Gómez Arrayás, J. C. Carretero, *Org. Lett.* **2020**, *22*, 6473–6478.
[58] M. J. Frisch, G. W. Trucks, H. B. Schlegel, G. E. Scuseria, M. A. Robb, J. R. Cheeseman, G. Scalmani, V. Barone, G. A. Petersson, H. Nakatsuji, X. Li, M. Caricato, A. V. Marenich, J. Bloino, B. G. Janesko, R. Gomperts, B. Mennucci, H. P. Hratchian, J. V. Ortiz, A. F. Izmaylov, J. L. Sonnenberg, D. Williams-Young, F. Ding, F. Lipparini, F. Egidi, J. Goings, B. Peng, A. Petrone, T. Henderson, D. Ranasinghe, V. G. Zakrzewski, J. Gao, N. Rega, G. Zheng, W. Liang, M. Hada, M. Ehara, K. Toyota, R. Fukuda, J. Hasegawa, M. Ishida, T. Nakajima, Y. Honda, O. Kitao, H. Nakai, T. Vreven, K. Throssell, J. J. A. Montgomery, J. E. Peralta, F. Ogliaro, M. J. Bearpark, J. J. Heyd, E. N. Brothers, K. N. Kudin, V. N. Staroverov, T. A. Keith, R. Kobayashi, J. Normand, K. Raghavachari, A. P. Rendell, J. C. Burant, S. S. Iyengar, J. Tomasi, M. Cossi, J. M. Millam, M. Klene, C. Adamo, R. Cammi, J. W. Ochterski, R. L. Martin, K. Morokuma, O. Farkas, J. B. Foresman, *GAUSSIAN 16 (Revision C.01) ed.*, Gaussian Inc., Wallingford, CT **2019**.
[59] T.-D. J. Stumpf, M. Steinbach, M. Höltke, G. Heuger, F. Grasemann, R. Fröhlich, S. Schindler, R. Göttlich, *Eur. J. Org. Chem.* **2018**, *2018*, 5538–5547.
[60] S. Pospisilova, J. Kos, H. Michnova, I. Kapustikova, T. Strharsky, M. Oravec, A. M. Moricz, J. Bakonyi, T. Kauerova, P. Kollar, A. Cizek, J. Jampilek, *Int. J. Mol. Sci.* **2018**, *19*, 2318.
[61] C. Zaugg, G. Schmidt, S. Abele, *Org. Process Res. Dev.* **2017**, *21*, 1003–1011.
[62] A. D. Skolyapova, G. A. Selivanova, E. V. Tretyakov, T. F. Bogdanova, L. N. Shchegoleva, I. Y. Bagryanskaya, L. Y. Gurskaya, V. D. Shteingarts, *Tetrahedron* **2017**, *73*, 1219–1229.
[63] P. Ravat, R. Hinkelmann, D. Steinebrunner, A. Prescimone, I. Bodoky, M. Juríček, *Org. Lett.* **2017**, *19*, 3707–3710.
[64] N. Sampathkumar, A. Murugesh, S. P. Rajendran, *J. Heterocycl. Chem.* **2016**, *53*, 924–928.
[65] C. Q. Meng, A. Long, S. Huber, S. R. Gurrala, D. E. Wilkinson, G. Pacofsky (MERIAL, INC.), US9249102B2 **2016**.
[66] M. J. Frisch, G. W. Trucks, H. B. Schlegel, G. E. Scuseria, M. A. Robb, J. R. Cheeseman, G. Scalmani, V. Barone, G. A. Petersson, H. Nakatsuji, X. Li, M. Caricato, A. V. Marenich, J. Bloino, B. G. Janesko, R. Gomperts, B. Mennucci, H. P. Hratchian, J. V. Ortiz, A. F. Izmaylov, J. L. Sonnenberg, Williams, F. Ding, F. Lipparini, F. Egidi, J. Goings, B. Peng, A. Petrone, T. Henderson, D. Ranasinghe, V. G. Zakrzewski, J. Gao, N. Rega, G. Zheng, W. Liang, M. Hada, M. Ehara, K. Toyota, R. Fukuda, J. Hasegawa, M. Ishida, T. Nakajima, Y. Honda, O. Kitao, H. Nakai, T. Vreven, K. Throssell, J. A. Montgomery Jr, J. E. Peralta, F. Ogliaro, M. J. Bearpark, J. J. Heyd, E. N. Brothers, K. N. Kudin, V. N. Staroverov, T. A. Keith, R. Kobayashi, J. Normand, K. Raghavachari, A. P. Rendell, J. C. Burant, S. S. Iyengar, J. Tomasi, M. Cossi, J. M. Millam, M. Klene, C. Adamo, R. Cammi, J. W. Ochterski, R. L. Martin, K. Morokuma, O. Farkas, J. B. Foresman, D. J. Fox, *GAUSSIAN 16 (Revision A.03) ed.*, Gaussian Inc., Wallingford, CT **2016**.
[67] T. B. Demissie, J. H. Hansen, *Dalton Trans.* **2016**, *45*, 10878–10882.
[68] T. B. Demissie, K. Ruud, J. H. Hansen, *Organometallics* **2015**, *34*, 4218–4228.
[69] M. Zhang, X. Lu, H.-J. Zhang, N. Li, Y. Xiao, H.-L. Zhu, Y.-H. Ye, *Med. Chem. Res.* **2013**, *22*, 986–994.
[70] T. Bruhn, A. Schaumlöffel, Y. Hemberger, G. Bringmann, *Chirality* **2013**, *25*, 243–249.
[71] R. Berrino, S. Cacchi, G. Fabrizi, A. Goggiamani, *J. Org. Chem.* **2012**, *77*, 2537–2542.
[72] C. Allais, O. Baslé, J.-M. Grassot, M. Fontaine, S. Anguille, J. Rodriguez, T. Constantieux, *Adv. Synth. Catal.* **2012**, *354*, 2084–2088.
[73] E. Debie, E. De Gussem, R. K. Dukor, W. Herrebout, L. A. Nafie, P. Bultinck, *ChemPhysChem* **2011**, *12*, 1542–1549.
[74] S. Grimme, J. Antony, S. Ehrlich, H. Krieg, *J. Chem. Phys.* **2010**, *132*, 154104.
[75] Version 1.1.0 Wavefunction ed., Inc. Irvine, CA, USA **2009**.
[76] J. J. P. Stewart, *J. Mol. Model.* **2007**, *13*, 1173–1213.
[77] G. A. Zhurko, Ivanovo (Russia) **2005**.
[78] R. D. Chambers, D. Holling, G. Sandford, A. S. Batsanov, J. A. K. Howard, *J. Fluorine Chem.* **2004**, *125*, 661–671.
[79] L. R. Faulkner, A. J. Bard, *Electrochemical methods: fundamentals and applications*, John Wiley and Sons **2002**.
[80] J. Tomasi, B. Mennucci, É. Cancès, *J. Mol. Struct.* **1999**, *464*, 211–226.
[81] P. J. Stephens, F. J. Devlin, C. F. Chabalowski, M. J. Frisch, *J. Phys. Chem.* **1994**, *98*, 11623–11627.

[82] E. L. Eliel, S. H. Wilen, *Stereochemistry of organic compounds*, John Wiley & Sons **1994**.
[83] A. D. Becke, *J. Chem. Phys.* **1993**, *98*, 5648–5652.
[84] C. Lee, W. Yang, R. G. Parr, *Phys. Rev. B* **1988**, *37*, 785–789.
[85] A. D. Becke, *Phys. Rev. A* **1988**, *38*, 3098–3100.
[86] T. Clark, J. Chandrasekhar, G. W. Spitznagel, P. V. R. Schleyer, *J. Comput. Chem.* **1983**, *4*, 294–301.
[87] S. H. Vosko, L. Wilk, M. Nusair, *Can. J. Phys.* **1980**, *58*, 1200–1211.
[88] A. D. McLean, G. S. Chandler, *J. Chem. Phys.* **1980**, *72*, 5639–5648.
[89] R. Krishnan, J. S. Binkley, R. Seeger, J. A. Pople, *J. Chem. Phys.* **1980**, *72*, 650–654.
[90] W. C. Still, M. Kahn, A. Mitra, *J. Org. Chem.* **1978**, *43*, 2923–2925.
[91] W. J. Hehre, R. Ditchfield, J. A. Pople, *J. Chem. Phys.* **1972**, *56*, 2257–2261.
[92] R. L. Soulen, D. G. Kundiger, S. Searles, R. A. Sanchez, *J. Org. Chem.* **1967**, *32*, 2661–2663.
[93] R. L. Gay, C. R. Hauser, *J. Am. Chem. Soc.* **1967**, *89*, 1647–1651.
[94] F. W. Cagle, H. Eyring, *J. Am. Chem. Soc.* **1951**, *73*, 5628–5630.

Manuscript received: April 19, 2023
Accepted manuscript online: May 24, 2023
Version of record online: July 25, 2023